Aharanov-Bohm oscillations of conductance in two-dimensional rings

Konstantin N. Pichugin and Almas F. Sadreev*
L. V. Kirensky Institute Physics, Krasnoyarsk 660036, Russia
and Åbo Academi, Institutionen för Fyzik, Department of Physics, Krasnoyarsk State University, Krasnoyarsk 660062, Russia
(Received 21 June 1996; revised manuscript received 22 May 1997)

Transport properties of mesoscopic rings with applied external magnetic field are considered numerically. Rings have square and circular forms and a finite aspect ratio d/L where L is the ring size and d is the width of ring arms. The type of the Aharonov-Bohm oscillations (ABO's) of the transmission substantially depends on the number of channels participating in the electron transmission. Moreover the aspect ratio and the geometrical form of the ring are important for the ABO's. In square rings with a small aspect ratio ($d/L=1/10$) the transmission displays periodic ABO's in the region of applied magnetic field defined by the inequality $\infty > l_B=(\hbar c/eB)^{1/2} \geqslant d$, while for rings with a large aspect ratio ($d/L=1/3$) only the single-channel transmission has quasiperiodical ABO's. For the circular rings with small aspect ratios the quasiperiodic ABO's are observed all over the region of the applied magnetic field while for the rings with moderate aspect ratios only the multichannel transmission displays irregular ABO's. The probability current flow patterns demonstrate fine correspondence between the transmission and the vortex structure of current distributions in the rings. For single-channel transmission, electron currents are laminar. For multichannel transport, current flow patterns display a complicated convection pattern in the form of a vortex lattice. An elementary cell of the vortex lattice consists of a few vortices and antivortices and has a size of $\sim d/f$, where f is the number of channels of electron transmission in the ring. Application of the flux distorts the vortex lattice enormously, partially destroying it. Correspondingly the Aharonov-Bohm oscillations of the transmission become irregular. [S0163-1829(97)02836-1]

I. INTRODUCTION

Transport properties of mesoscopic structures and nanostructures in the form of quantum wires, dots and wells, heterostructures and so on attract much attention because of rapid development of nanotechnology with the use of methods of molecular beam epitaxy and lithography.[1] These methods can fabricate such perfect structures that the observed transport properties are defined mostly by the quantum-mechanical coherence of electrons over the whole structure. In these structures the magnetic field can tune the phase of the electronic wave function by the value $(e/\hbar c)\int d\mathbf{r}\mathbf{A}$. If an electron can pass two different trajectories, at the place of crossing of the trajectories the phase shift is given by $2\pi\gamma$, where

$$\gamma = \frac{\Phi}{\Phi_0}, \tag{1}$$

$\Phi = BS$ is the magnetic flux enclosed by these trajectories with area S, and $\Phi_0 = 2\pi\hbar c/e$ is the flux quantum.[2,3] Therefore, in the case of the one-dimensional ring with two leads the transport properties of electrons should be periodical with the period $\gamma = 1$. This type of oscillation is referred to as Aharonov-Bohm oscillations (ABO's).

Obviously, the backscattering processes which can take place in the arms of the ring due to, for example, impurities or geometry of the ring may change the type of the ABO's. It has been believed, that the ABO's should vanish once the elastic mean free path of the electron is smaller than or of the order of the system's size. However, Al'tshuler *et al.*[4] predicted the ABO's in highly disordered systems the ABO's of magnetoresistance with the period 1/2. This is believed to be the result of some kind of coherent backscattering associated with localization. Later, in Refs. 5–7 the transmission probability between two terminals of the one-dimensional ring with two arbitrary scatterers was calculated exactly as a function of the flux. The period of the ABO's was found to be Φ_0 , though for weak scattering higher harmonics may develop. Gefen *et al.*[6] found specific conditions on the parameters of scatterers to enhance the effect of the second harmonic and produce the effective ABO's period $\Phi_0/2$. Similar results were obtained in Ref. 8 where the processes of elastic scattering of electron by phonons were modeled by the time-periodic flux. In Refs. 9 and 10 it was demonstrated with the help of modeled disorder that to observe only the $\Phi_0/2$ component of the ABO's in the single ring experiments it is necessary to perform ensemble disorder averaging. Moreover, Büttiker *et al.*[11] considered the the multichannel conductance of the one-dimensional ring and obtained the dependence on channel number N of the contributions to the conductance. They found that the terms with period Φ_0 and period $\Phi_0/2$ vary with N as $1/N$.

In reality, in experiments on very small rings of gold with circumference $\sim 100-500$ nm and width ≈ 40 nm no strictly periodic behavior of any kind was observed.[12–15] Basically magnetoresistance oscillations have the ABO's period Φ_0 and the period $\Phi_0/2$ as a harmonic. Besides, the Fourier transformation of the flux dependence of the magnetoresistance reveals the contribution of the aperiodic fluctuations. The detailed structure of the Φ_0 peak in the power spectrum is, as it was suggested by Stone,[16] the result of mixing of the field scales corresponding to the area of the hole in the ring and the area of the arms of the ring. Actually, with decreas-

ing of the aspect ratio d/L, where d is a width of the arms and L is a size of the ring, the contribution of the aperiodic fluctuations increases.[12,13] The first numerical analysis of quantum fluctuations of the magnetoresistence of the two-dimensional strip in the framework of the hopping model with random site energies was performed by Stone.[16] It was shown that the stationary fluctuations of the magnetotransport of electrons are a direct consequence of the microscopic quantum states in specific samples. These fluctuations enhance much if the states become localized. Magnetotransport in the two-dimensional tight-binding model of a strip was also numerically considered recently in Ref. 17. It was shown that the ''Hofstadter's butterfly'' structure of the spectrum of energy levels of the strip gives rise to the fractal structure in the field and energy dependence of the conductance.

Similarly, in application to the quantum Hall effect it was shown that strong quantum fluctuations of the low-temperature conductance arise because of resonant transmission of the electrons through the localized states of the sample.[18–20] In the work of Shapiro,[21] it was found that corrections to the quantum Hall effect in a straight electron waveguide have a value of the order $(d/l_B)^2$, where

$$l_B=\left(\frac{\hbar c}{eB}\right)^{1/2}, \tag{2}$$

is the magnetic length. Experimental investigations of the quantum Hall effect in many-terminal mesoscopic rings show the deviation from exact quantization in the form of the aperiodic fluctuations at low magnetic field.[22] The authors conclude that these fluctuations arise from Aharonov-Bohm interference effects as the electrons are elastically scattered by impurities or geometric features.

Dirac[23] and later Hirschfelder *et al.*[24–26] have shown that quantum-mechanical probability currents (streamlines) can form vortices around the nodes of the wave functions. Recently, an interest to current vortices was resumed in the series of works in which the electron transport was considered numerically in two-dimensional quantum wires. Specifically, the vortical current flows were found in straight wires with impurities,[27–29] in a model crossbar structure,[30] in multiple-bend wires,[31–33] two-dimensional structures with curvilinear boundaries[34,35] and straight wires with potential barrier inside them.[36,37] The current vortices result in new peculiarities in the quantum Hall effect because they form edge states near the boundaries of the two-dimensional structures. The edge states provide perfect transmission of electrons in spite of impurities. Moreover, as it was found by Berggren and Ji[31] the vortex structure of the current state is responsible for a change of the laminar regime of electron transport to the convectional one in the quantum wire with two knees.

A consideration of the conductance oscillations in the circular quasi-one-dimensional ring with a small aspect ratio in the ballistic regime was calculated by Shin *et al.*[38] with the help of the scattering matrix. In this work we numerically consider transport properties of square and circular rings with finite aspect ratios connected with two leads in single electron approximation and in the ballistic regime. An external magnetic field applied normally to the plane of the ring is considered to be homogeneous over the whole ring structure plus leads. Similar to Ref. 38, we use the hard-wall approximation for the electron confinement inside the structure. This approximation is justified if the Fermi energy of the transport electron is much smaller than the confinement potential. The main attention is given ABO's of the transmission to demonstrate how the ABO's are ''deteriorated'' with increasing aspect ratio d/L and a number of electron transport channels.

We solve the Schrödinger equation numerically in the framework of the two-dimensional tight-binding model to find the ABO's of the conductance and detailed current flow distributions. However, we are restricted by the field region where one flux quantum per lattice plaquette is much less than unity, which makes the continual Schrödinger equation certainly applicable. The current flow patterns display rich vortex structures and show that the formation of the convectional vortex flow patterns is directly related to the complexity in flux dependence of the transmission. We show that the laminar flow of the electron takes place only in the very restricted case of the rings with small and moderate aspect ratios, with the single-channel transport, and with zero flux. Application of the flux gives rise to the current vortex near the entrance of the ring. This vortex mixes inner and outer paths of the electron transport in such a way that phase shifts induced by different fluxes enclosed by different trajectories of the electron in the ring become equaled. As a result we can observe the quasiregular ABO's of the transmission in rings with small aspect ratios. With an increasing in the aspect ratio and the number of channels the ABO's of the transmission become irregular and, correspondingly, the current flow patterns acquire a rather volatile form with complex distribution of vortices.

II. BASIC EQUATIONS

We begin a consideration with the square two-terminal ring. For simplicity we take a width of leads equaled to the width of the ring's arms d. The Schrödinger equation in the single-electron approximation has the following form:

$$\left[\frac{1}{2m}\left(\mathbf{p}-\frac{e}{c}\mathbf{A}\right)^2+V(\mathbf{x})\right]\psi(\mathbf{x})=E\psi(\mathbf{x}), \tag{3}$$

where a vector potential in the Landau gauge is defined as

$$\mathbf{A}=(-By,0,0), \tag{4}$$

$V(x)$ is the potential confined electron inside the ring. The Fermi energy for the metal ring or the chemical potential for the semiconductor one is supposed to be constant over the whole structure including the gates. The magnetic field is supposed to be applied normally to the whole structure with the gates included.

Let us introduce the dimensionless coordinates $x\rightarrow x/d$. Then Eq. (3) takes the following form:

$$\left[\left(i\frac{\partial}{\partial x}+\gamma y\right)^2-\frac{\partial^2}{\partial y^2}\right]\psi=\epsilon\psi, \tag{5}$$

with the dimensionless flux

$$\gamma=2\pi Bd^2/\Phi_0, \tag{6}$$

and the dimensionless energy

$$\epsilon = 2md^2E/\hbar^2. \tag{7}$$

The transmission probability which defines the conductance of the structure in accordance with the Landauer-Buttiker formula,[39,40] can be found by different ways.[42,31,38,43,44] Here we consider the solution in the input lead as follows:

$$\psi_{\rm in}(x,y) = e^{i\kappa x}\phi_1(y) + \sum_f a_f e^{-i\kappa_f x}\phi_f(y), \tag{8}$$

where the y axis is assumed to be orthogonal to the lead, and $\phi_f(y)$ are solutions of one-dimensional equation,

$$\left[(\kappa_f + \gamma y)^2 - \frac{\partial^2}{\partial y^2}\right]\phi_f(y) = \lambda_f \phi_f(y), \tag{9}$$

with zero boundary condition on walls of the lead.

$$\epsilon = \kappa_f^2 + \lambda_f. \tag{10}$$

All wave numbers κ, κ_n are dimensionless via the width of the lead. The outgoing solution can be presented as follows:

$$\psi_{out}(x,y) = \sum_f b_f e^{-i\kappa_f x}\phi_f(y). \tag{11}$$

Inside the ring we solve numerically the two-dimensional Schrödinger equation:

$$(4-\epsilon)\psi_{m,n} - e^{i\gamma n}\psi_{m+1,n} - e^{-i\gamma n}\psi_{m-1,n} - \psi_{m,n+1} - \psi_{m,n-1} = 0, \tag{12}$$

where m and n run from 1 to N. This numerical Schrödinger equation is equivalent to the two-dimensional tight-binding model used in Ref. 17 for describing of magnetotransport in stripes. However, we are restricted by the flux region and sizes of the numerical lattices for which lattice effects are considered to be not important. The solution of Eq. (12) starts from the boundary between the lead and the ring where $\psi(m,0) = \psi_{\rm in}(x_m,0)$, or top the edge points of the ring where $\psi(m,0) = 0$, then continues inside the ring and terminates at the boundary between the ring and the output lead where $\psi(m,N+1) = \psi_{\rm out}(x_m,L)$, or down the edge points of the ring where $\psi(m,N+1) = 0$. As a result, we obtain a system of equations for the coefficients a_f, b_f which determine the transmission and reflection probabilities as follows:

$$T = \sum_{f=1} \frac{Re(\kappa_f)}{\kappa}|b_f|^2, \quad R = \sum_{f=1} \frac{Re(\kappa_f)}{\kappa}|a_f|^2. \tag{13}$$

An accuracy of calculation was controlled by a condition that $T+R=1$ which was satisfied within computer error 10^{-15}.

To consider the multichannel conductance of the two-terminal ring we rewrite the input wave function (8) of electron incident in channel j and the output wave function (11) as follows:[40,41]

$$\psi_{{\rm in},j}(x,y) = e^{i\kappa_j x}\phi_j(y) + \sum_f a_{fj} e^{-i\kappa_f x}\phi_f(y), \tag{14}$$

$$\psi_{{\rm out},j}(x,y) = \sum_f b_{fj} e^{-i\kappa_f x}\phi_f(y). \tag{15}$$

Then using Landauer's formula[39,40] the conductance can be written as follows:

$$G = \frac{e^2}{h}\sum_{f,j} (\kappa_f/\kappa_j)|b_{fj}|^2. \tag{16}$$

Next, we calculate the current distributions

$$\mathbf{j}(x,y) = \frac{ie\hbar}{2m}(\psi\nabla\psi^* - \psi^*\nabla\psi) - \frac{e^2}{mc}\mathbf{A}|\psi|^2. \tag{17}$$

In computer simulations formula (14) takes the following form taking into account gauge (5):

$$\frac{j^{(x)}_{m,n}}{j_0} = i[\psi^*_{m,n}e^{i\gamma n}\psi_{m+1,n} - \text{c.c.}],$$

$$\frac{j^{(y)}_{m,n}}{j_0} = i[\psi^*_{m,n}\psi_{m,n+1} - \text{c.c.}], \tag{18}$$

where

$$j_0 = \frac{e\hbar}{2md}.$$

In the circular ring we use the same equations as for the square ring except for boundaries. The boundary conditions for the circular ring have the following form:

$$\psi(m,n) = 0 \quad \text{if} \quad R_1^2 \geqslant n^2 + m^2 \geqslant R_2^2. \tag{19}$$

III. NUMERICAL RESULTS. AHARONOV-BOHM OSCILLATIONS OF THE CONDUCTANCE

A. Square ring

First, we consider the rings with small aspect ratio $L \gg d$. Specifically, in terms of numerical lattice we chose three types of the aspect ratio: $d/L = 1/10$, $d/L = 1/5$, and $d/L = 1/3$. Magnetic flux dependences of the total transmission defined by formula (14) and the conductance defined by formula (16) are given in Figs. 1–3 for different energies of the incident electron ϵ. The values of the energy correspond consequently to the one-, two-, and three-channel electron transport in the leads with $f = 1,2,3$. In the dimensional units in accordance with formula (6) the energy $\epsilon = 20$ (the single-channel transmission) for the metal ring can be achieved for $d \sim 1$ nm provided that the Fermi energy is of order of 1 eV, while an electron transmitting in the lead with the width $d \sim 10$ nm has the energy $\epsilon \sim 200$. For the semiconductor structure on the basis of GaAs where the Fermi energy is of an order of 50 meV and the effective mass of the electron $m^* \approx 10^{-28}$,[45,46] we obtain that the width of the semiconductor waveguides may range from $d \sim 10$ nm (the single-channel transmission) to $d \sim 100$ nm (three- and multi-channel transmissions).

To show the ABO's period we have introduced the dimensionless flux as a ratio of the flux through the mean area of the ring to the flux quantum,

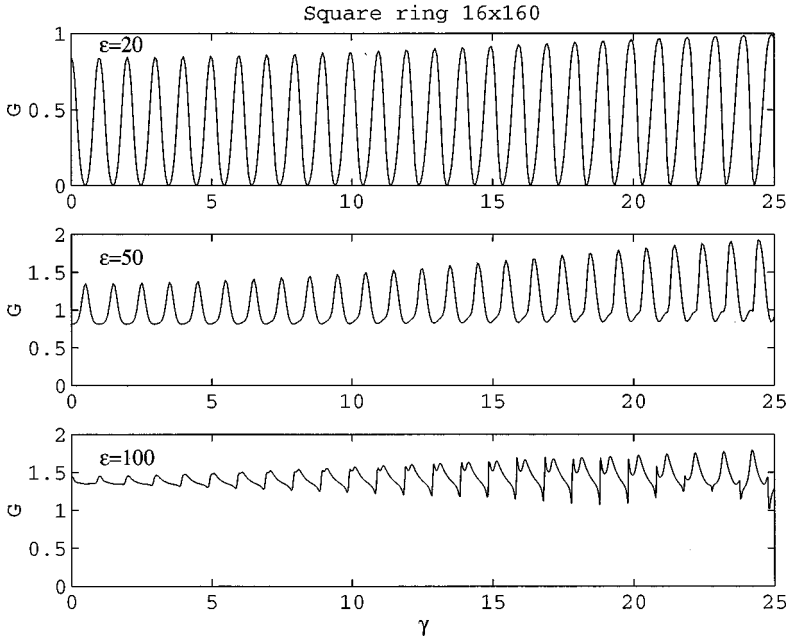

FIG. 1. The Aharonov-Bohm oscillations (ABO's) of the conductance G through the square ring with small aspect ratio $d/L=1/10$ (16×160 in lattice scale). Notation $m\times n$ means that m is numerical width of arms of the ring and n is the ring's size. The flux γ defined by formula (20) is a ratio of the magnetic flux through the mean area of the ring to the flux quantum. (a) The transmission with the energy $\epsilon=20$ which coincides with the conductance in this case; (b) the transmission and the two-channel conductance with $\epsilon=50$; (c) the transmission and the three-channel conductance with $\epsilon=100$.

$$\gamma=\frac{\Phi_{\square}}{\Phi_0}=\frac{B(L-d)^2}{\Phi_0}=\frac{\widetilde{\gamma}(L-d)^2}{d^2}, \tag{20}$$

where $\widetilde{\gamma}$ is defined in Eq. (1). In the limit $d\to0$ the ABO period $\widetilde{\gamma}\to1$.

The single-channel transmission. We begin by considering the single-channel input wave function (8). In Fig. 1 the ABO's of the transmission coinciding with the conductance are shown for the case of small aspect ratio $d/L=16/160=1/10$. Numbers 16 and 160 mean numerical lattice sizes of the ring. These numbers were optimized in such a way that an increase in the lattice sizes does not give any visible changes in the transmission. The metal rings measured by Webb *et al.*[12] with $L=825$ nm, $d=41$ nm, and $In_xGa_{1-x}As/InP$ rings measured by Appenzeller *et al.*[47] with $L=700$ nm, $d=85$ nm belong to this type of ring with a small aspect ratio. The metal ring measured by Webb *et al.*[12] with $L\approx282$ nm, $d=37$ nm approximately belongs to the type of rings with a moderate aspect ratio which is shown in Fig. 2 ($d/L=24/120=1/5$). As it is seen from Figs. 1–3 the single-channel transport display only the periodic ABO's for the ring with a small aspect ratio while for the ring with a moderate aspect ratio there are three characteristic regions of the ABO's of the transmission which depend on the aspect ratio.

The region of periodic sinusoidal ABO's is the first. The smaller the aspect ratio and the less the number of channels, the wider the region of periodic sinusoidal ABO's. Also for some values of the energy of an incident electron the ABO's can contain the second harmonic as is shown in Fig. 10 for the circular ring. A discussion of this phenomenon is given in subsection B. For the single-channel transmission and for any aspect ratio this region shown in Figs. 1–3 can be ap-

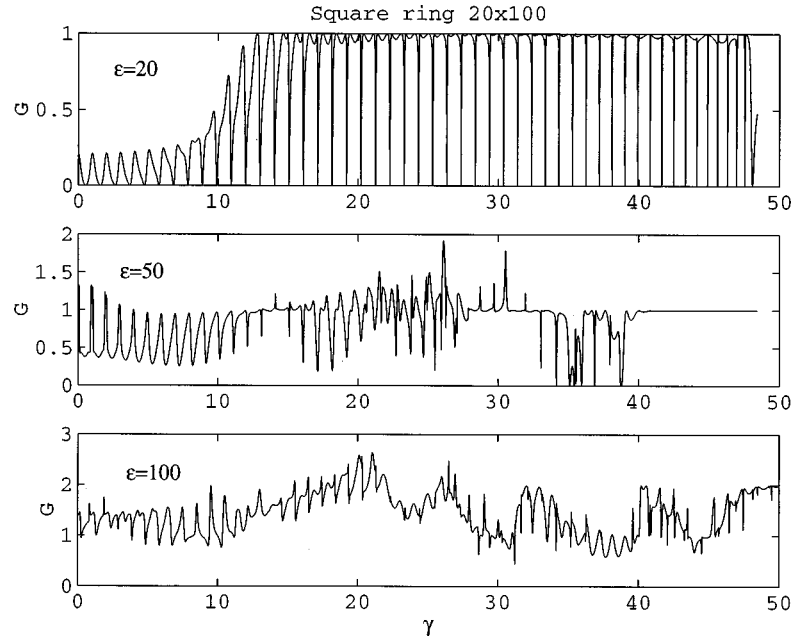

FIG. 2. The same as in Fig. 1 for the aspect ratio $d/L=1/5$ (20×100 for $\epsilon=20$ and 24×120 for $\epsilon=50,\ 100$).

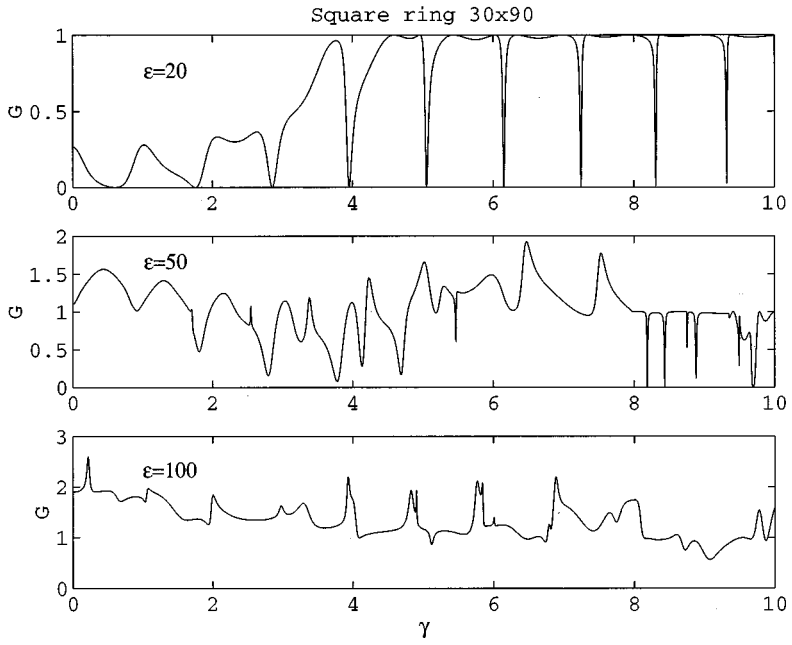

FIG. 3. The same as in Fig. 1 for the aspect ratio $d/L=1/3$ (30×90 ring).

proximately defined in terms of the magnetic length (2) as $d/\sqrt{2}\leqslant l_B$, where it is convenient to express l_B via magnetic flux γ as follows:

$$l_B=d\sqrt{\frac{1}{\tilde{\gamma}}}=d\sqrt{\frac{1}{2\pi\gamma}}\frac{(L-d)}{d}. \tag{21}$$

The first peculiarity, which can be seen from Figs. 1–3, is that the maxima of the single-channel transmission are less than unit in the first flux region. The reason for this is resonant transmission through the ring as it is shown in Fig. 4(a). Peaks of the transmission are caused by a packing of wavelengths inside the ring. Because of complicated geometry of the square ring this packing is not so simple in comparison with the case of the circular ring [Fig. 4(b)]. It is clear that if we tuned to the resonant value of the energy maxima of the ABO's of the single-channel transmission it would be near unity.

Exact zeroes of the single-channel transmission at points $\gamma\approx m+1/2$, $m=0,1,2,\ldots$ are the next peculiarity in the region of regular sinusoidal ABO's. The electrons traversing the inner and outer perimeters acquire different phases from the magnetic field because the trajectories enclose different amounts of the flux.[16] It would mean that there would be no complete π interference in the ring with a finite aspect ratio. Actually, these arguments are correct provided that the electron trajectories are completely laminar. But current flow patterns for different fluxes over the ABO's period reveal that the electron trajectories are laminar only for $\gamma\approx m$, $m=0,1,2,\ldots$ [see Fig. 5 (the first subplot)]. With a deviation of the flux γ from the integer near the entrance to the ring a vortex appears (Fig. 5). As a result, the trajectories

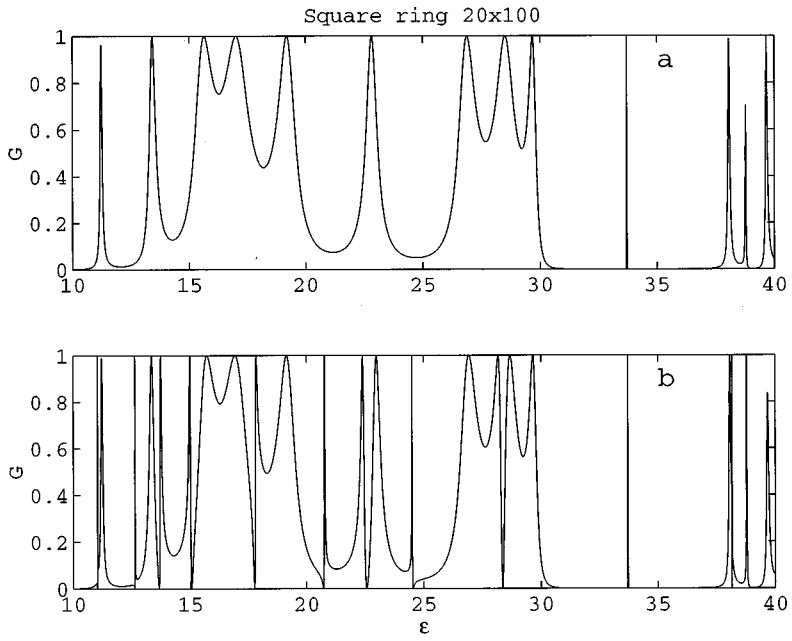

FIG. 4. The energy ϵ dependence of the transmission in the 20×100 square ring for the $\gamma=0$ (a) and $\gamma=0.08$ (b).

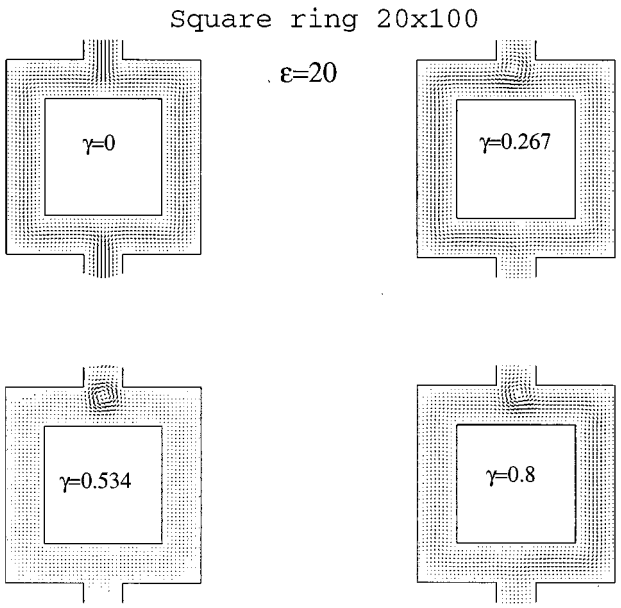

FIG. 5. Flux evolution of probability current distributions over the first sinusoidal ABO period for the single-channel transmission through the 20×100 square ring. The flux dependence of the transmission for this ring is shown in Fig. 2 (top subplot).

included into the vortex state enclose the small amount of flux opposite to the trajectories along the ring's arm. The chirality of the vortex chooses the ring's arm along which the prevailing current flows in such a way that the vortex trajectories and the trajectories along the ring's arms always have opposite captured fluxes. Moreover the greater the vortex currents the smaller the arm's ones. Finally, at the points $\gamma\approx m+1/2$ the vortex completely suppresses the arm's current to switch off the electron transmission through the ring. For this flux the current flow becomes degenerate relative to the direction of the flow and the vortex chirality changes sign. The phenomenon of a swift reversal of the vortices in the current distribution was found by Berggren and Ji[31] in the electron waveguides with circular bends just below the conductance dip without external magnetic field. While the current flow undergoes dramatic changes over the ABO's period the structure of wave functions $|\psi(x,y)|$ performs small periodical displacements near the electrodes of the ring.[48]

The second flux region is the region of the nonsinusoidal ABO's of the single-channel transmission where the magnetic length becomes less than the width of the ring's arms. In this region the maxima of the ABO's increase with a decrease in the magnetic length and reach unity for the transmission. At last, in the third region where $l_B \ll d$ the transmission is close to saturation everywhere over the flux except extremely narrow regions where the transmission falls to zero. As it is shown in Fig. 6 we observe semiclassical current distributions and the wave functions in the form of edge states. Note, that the aspect ratio of the ring has no noticeable influence on the estimations for the single-channel transmission, therefore they are universal.

Multichannel transmission. One can see that for the multichannel transmission the flux region of regular sinusoidal ABO's dissappears for the moderate and large aspect ratios, as it is seen from Figs. 2 and 3. Moreover, the multichannel conductance in these rings becomes practically irregular. The Fourier spectra of the ABO's of the conductance demonstrate how with an increase in the number of channels every Fourier peak acquires quasicontinual components (Fig. 7). It indicates that the ABO of the multichannel transmission in the rings with a moderate aspect ratio becomes irregular.

The quantum-mechanical streamline patterns presented in subplots of Fig. 8 show a substantial difference between the single-channel transport of the electron and the multichannel one in the ring. The streamlines are analogous to the classical trajectories[24,26] and are lines tangential to the current flows. For the multichannel transition there are nodal lines of the wave function which are both orthogonal and parallel to the ring's arms. Consequently, we obtain the current flows which form a convectional picture. The flow patterns form a

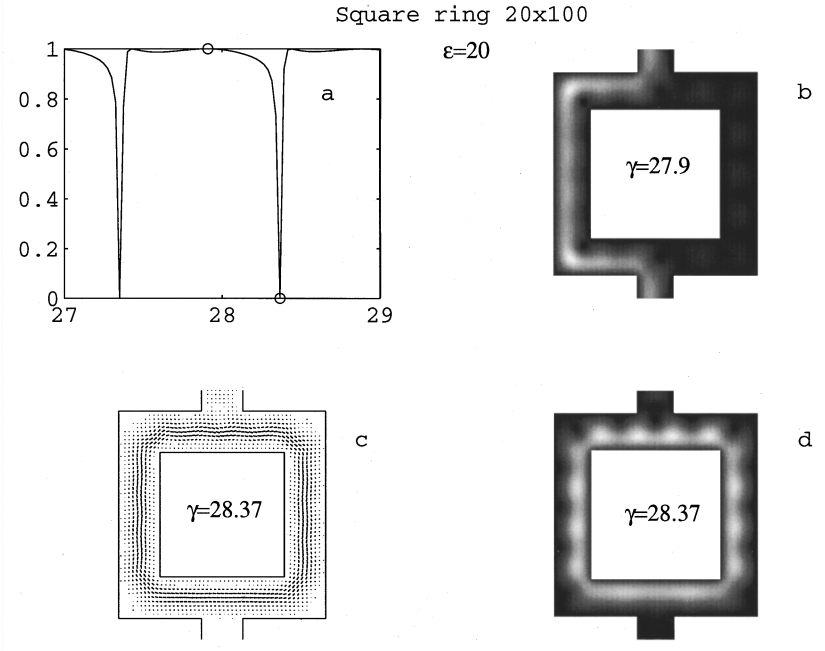

FIG. 6. Flux evolution of probability current distributions and the electron wave function $|\psi(x,y)|$ in the flux region where the magnetic length l_B is less than the ring width d. The flux values shown in subplots are indicated by open circles in (a).

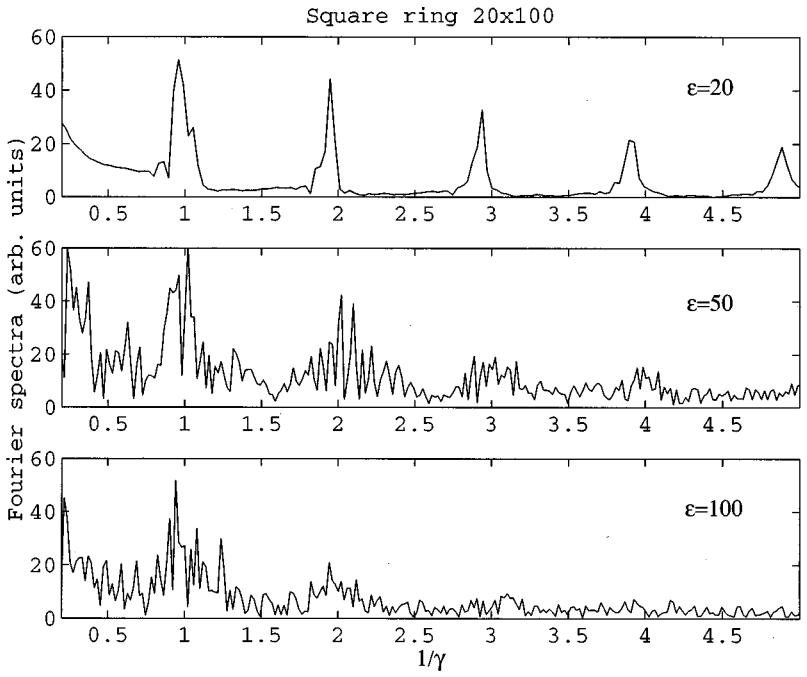

FIG. 7. The Fourier spectra of the flux dependence of the conductance in the square ring with the aspect ratio 1/5.

vortical lattice with an elementary cell consisting of a pair of vortices and one antivortex for $\gamma=0$. Application of the flux drastically deforms the vortical lattice as it is shown in subplots of Fig. 8. A small variation of the flux from zero to $\gamma=0.066$ practically destroys the convectional lattice to give the transmission equal unity. The further increase in the flux to $\gamma=0.13$ again gives rise to the convectional structure of the streamlines, which however, flow mostly inside the ring (the fourth subplot in Fig. 8). As a result the transmission becomes equal zero.

B. Circular rings

In the forthcoming figures the results of computer simulations of the transmission through the circular ring are presented. They are based on the the same equations as for the square ring except boundary conditions given by Eq. (19). Similar to the square ring it is convenient to introduce a dimensionless flux as a ratio of the flux through the mean area of the ring to the flux quantum,

$$\gamma=\frac{\Phi_{\rm circ}}{\Phi_0}=\frac{B\pi(R_2-d/2)^2}{\Phi_0}=\frac{\tilde{\gamma}\pi(R_2-d/2)^2}{d^2}, \qquad (22)$$

where $\tilde{\gamma}$ is defined in Eq. (1) and $d=R_2-R_1$.

As the circular ring has no rectangular corners in contrast to the square ring, we have smooth potential releif inside the ring. Actually the energy dependence of the transmission (Fig. 9) shows almost periodical oscillations up to the energies not exceeding $4\pi^2$ ($\sqrt{3}\pi$ in terms of the wave number). Each peak of the transmisison corresponds to a packing of an integer number of wavelengths inside the arms of the circular ring. However, in the range of the energies where the second

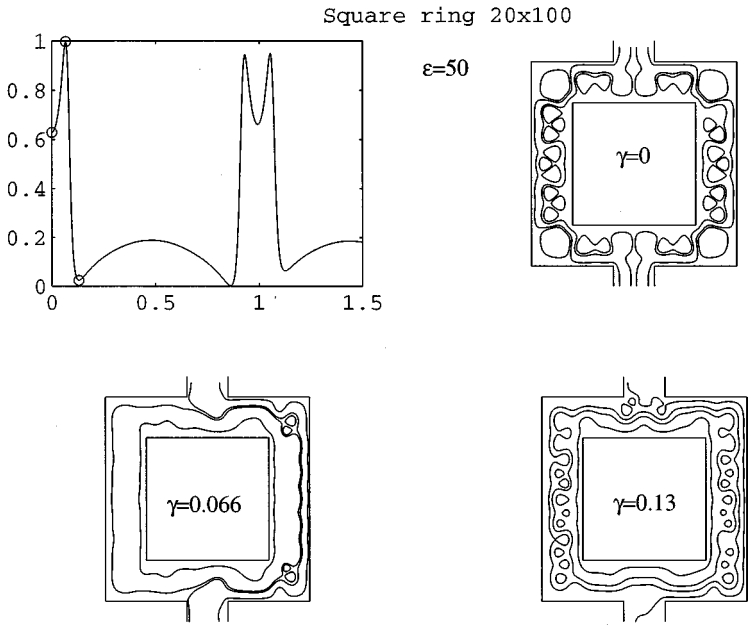

FIG. 8. Flux evolution of probability current distributions over the first ABO period for the two-channel transmission through the 20×100 square ring. The flux values shown in subplots are indicated by open circles in the first subplot.

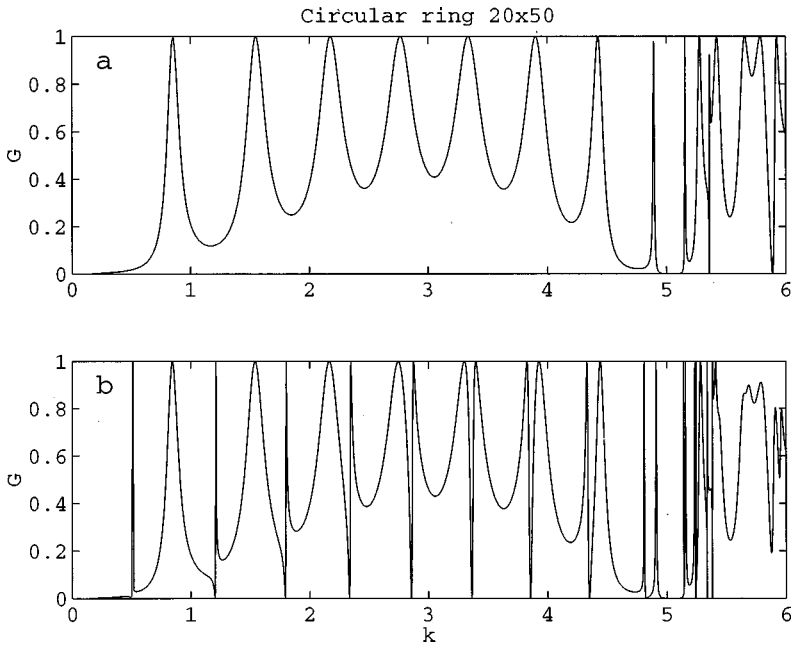

FIG. 9. The energy ϵ dependence of the transmission in the 20×50 circular ring for the $\gamma=0$ (a) and $\gamma=0.08$ (b). Notation $m\times n$ is the numerical width of the ring's arms and the outside radius correspondingly.

channel of transmission participates, the energy dependence of the transmission becomes complex. This is due to the fact that the radial packing of the wave function inside the ring gives rise to new additional peaks of the transmission, the energy position of which is incommensurate to the peaks of the transmission due to the azimuthal packing. As a result, we see quite irregular behavior of the transmission peaks in Fig. 9(a) for high energies of the incident electron. An involvment of new channels of the electron transmission inside the rings gives rise to a further complication of the transmission peaks. Correspondingly, the ABO's of the transmission are extremely dependent on the number of channels of the electron transmission.

In the second subplot of Fig. 9(b) we see that an application of the flux induces new peaks of the transmission, the form of which, however, differs from the peaks shown in Fig. 9(a). Similar behavior of the energy dependence takes place for the square rings (Fig. 4). This phenomenon of the flux induced resonant transmission through the ring was first considered for the one-dimensional rings.[49] The explicit form of the flux induced resonant peaks was obtained which near the nth peak has the following form:

$$G(\epsilon,\gamma)=\frac{1}{1+\left\{\dfrac{\pi^2\gamma^2}{\epsilon_n-\epsilon}-2\Gamma\right\}^2}, \tag{23}$$

where Γ is a parameter defined by contact of the ring with the leads.

The nature of the flux induced resonant transmission in the two-dimensional rings was discussed in Ref. 50. Consider the transmission of the incident electron through the ring with the leads as the transmission through a resonant cavity, consisting of the ring plus two symmetrical bars as contacts. For a weak coupling of this resonant cavity with the leads the transmission is resonant and takes place if the energy of the incident electron is close to the quasienergies of the resonant cavity. The width of the resonant transmission is defined by the width of the quasienergy which in turn depends on coupling of the resonant cavity with the leads. Positions of quasienergies are given by eigenvalues of the resonant cavity. A half of the corresponding eigenfunctions is symmetric with respect to $y\rightarrow -y$ and the other half of the eigenvalues is antisymmetric, where the y axis is orthogonal to the leads. So, if the incident wave function is symmetric with respect to $y\rightarrow -y$ as it takes place for the first-channel transmission and the flux equaling zero, only the quasienergy states with the same symmetry are transparent for the incident electron. It is a case of the transmission, which is shown in Fig. 9(a). Application of the flux violates the symmetry of the incident wave function to give rise to new peaks of the resonant transmission through the antisymmetric states of the cavity. This phenomenon is shown in Fig. 9(b). Since for the small flux a distortion of the incident wave function can be considered by the perturbation theory and as proportional to γ^2, correspondingly, the width of the flux induced peaks of the resonant transmission is also proportional to γ^2, as is seen from formula (23).

If to draw the transmission probability through the two-dimensional circular ring as a function of the flux and the energy (Fig. 10, first subplot), we can observe a good coincidence of the plot with the energy levels of the resonant cavity consisting of the ring plus two bars.[50] Also one can see from Fig. 10 that a choice of the energy of the incident electron defines the type of the ABO's. Specifically, if to take the energy slightly exceeding the symmetrical quasienergies, the transmission decreases with the application of the flux $[(\delta G/\delta\gamma)<0]$, and we obtain the almost sinusoidal ABO's. Otherwise, for the energies of the incident electron, for which $\delta G/\delta\gamma>0$, we obtain the ABO's consisting of two harmonics. Particular behavior of the derivative $\delta G/\delta\gamma$ is shown in the second subplot of Fig. 10, where two vertical lines indicate the cases of the negative ($\epsilon=15$) and positive ($\epsilon=16$) derivative. Therefore, the number of harmonics in the ABO's for the first-channel transmission is defined by the energy of the incident electron. If the energy is above the even quasienergy, the ABO's contains one harmonic. If the the energy of the incident electron is spaced between the

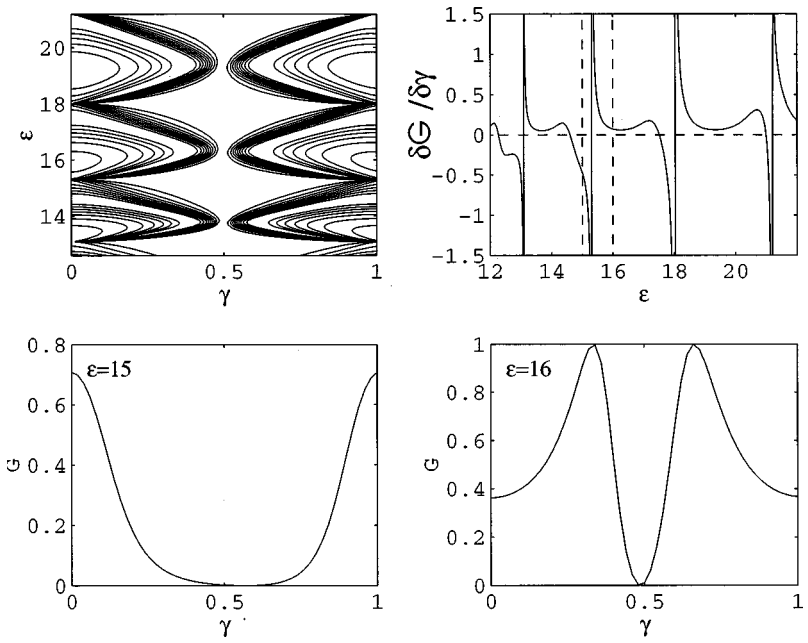

FIG. 10. The transmission probability through the 20×50 circular ring as a function of the flux and the energy plotted in the form of contour lines in the first subplot. The second subplot shows the energy dependence of derivative $\delta G/\delta\gamma$ for $\gamma=0.02$, the sign of which defines the number of harmonics in the ABO's for the first-channel transmission presented in the third and fourth subplots.

even quasienergy and odd one the ABO's contains at least two harmonics. Both types of the ABO's are shown in the next subplots of Fig. 10. The origin of the high harmonics in the ABO's was discussed in many works for the one-dimensional and quasi-one-dimensional rings[5–10,16,38,51–53] using different approaches. Present consideration of the transmission through the two-dimensional rings reveals purely geometrical origin of the other periodicity of the ABO's based on symmetry arguments of the structure.[50]

The flux dependence of the quasienergies, which approximately coincides with the plot of the transmission given in the first subplot of Fig. 10 governs the behavior of the current flows in the ring by formula $j\sim-\partial\epsilon/\partial\gamma$. These current flow patterns are shown in Fig. 11. In the first subplot for $\epsilon=15.2$ the derivative is negative, and the current flows mostly in the left arm of the ring. In the fourth subplot for $\epsilon=15.4$ the derivative is positive, and the current flows mostly in the right arm. The second and third subplots demonstrate current flow patterns for the case $G=0$ and $G=1$, respectively.

As it was discussed above, whether or not the ABO's of the conductance are regular is defined by the aspect ratio and the number of channels of the transmission inside the ring. For the single-channel transmission the periodic ABO's in the circular ring take place for the small and moderate aspect ratios. For the ring with a small aspect ratio (Fig. 12) the two- and three-channel conductance displays many sets of the periodical ABO's. However, for the circular ring with a large aspect ratio ($d/R=0.5$, Fig. 13) even the two-channel transmission reveals practically irregular ABO's of the conductance. The Fourier spectra of the ABO's of the conductance of the circular ring have the form similar to that in the square ring (Fig. 7), so they are not shown here. Therefore, the phenomenon of irregularity in the ABO's of the transmission of the electron through the rings with the finite aspect ratio is universal and does not depend on the geometry of rings.

Figure 14 demonstrates a transition of the current distribution from laminar to the convectional regime with the formation of the azimuthal vortex lattice with an increase in energy of the incident electron. For $k=4.89$ there are only vortices near the entrance to the ring while for $k=6.32$ the convectional lattice of the vortices forms inside the ring. In Ref. 54 similar convectional structures were demonstrated for circular billiard. As a result, the electron trajectories for the multichannel transport become rather volatile provided that the magnetic length exceeds the arm's width. It leads to an enormous phase shift by the external flux for these trajectories which pass between the vortex cells. Correspondingly, at the moment of meeting of the trajectories in the down electrode the phase difference can be rather unpredictable

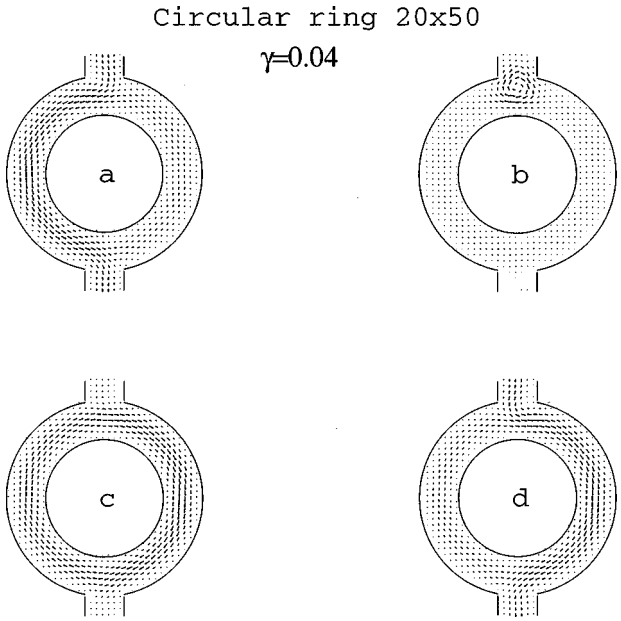

FIG. 11. The energy evolution of probability current distributions for the first-channel transmission through the 20×50 circular ring is shown. The first subplot (a) $\delta G/\delta\gamma<0$. The second subplot (b) $G=0$. The third subplot (c) $G=1$. The fourth subplot (d) $\delta G\,\delta\gamma>0$.

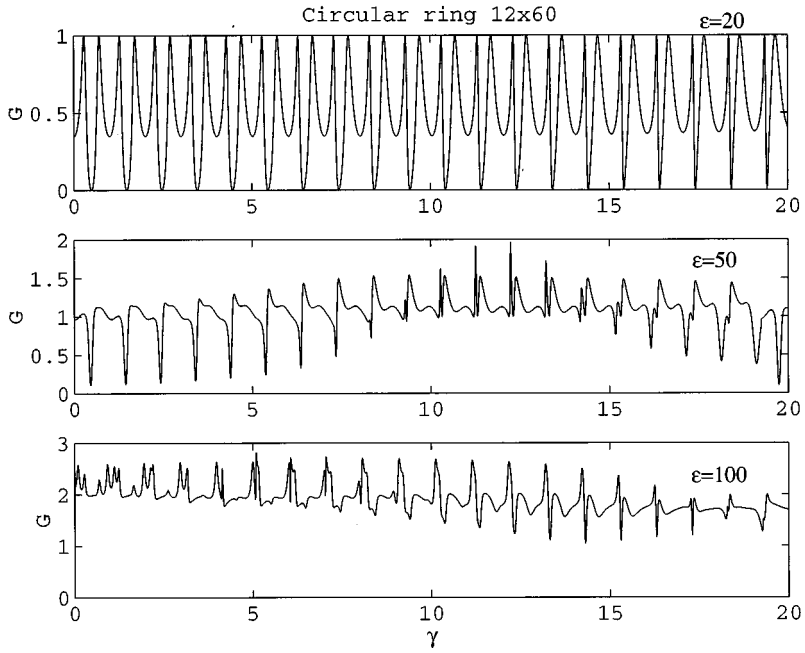

FIG. 12. The Aharonov-Bohm oscillations (ABO) of the transmission through the circular ring with the small aspect ratio $d/L=0.1$ (12×60 ring in lattice scale). The flux γ defined by formula (22) is a ratio of the magnetic flux through the mean area of the ring to the flux quantum. (a) The single-channel transmission with the energy $\epsilon=20$; (b) the two-channel transmission with $\epsilon=50$; (c) the three-channel transmission with $\epsilon=100$.

depending on the place of meeting, leading to nonregular oscillations of conductance as a function of the flux. In order to demostrate this instability of incident trajectories inside the ring in Fig. 15 we show the streamlines. At the left of Fig. 15 one can see that for the single-channel transmission the trajectories which are numerically closest (the horizontal distance between them is taken as equal to the lattice unit) in the input lead are stable inside the ring. However, for the four-channel transmission the two closest incident streamlines acquire finite phase differences of an order of fR, where f is the number of channels.

IV. CONCLUDING REMARKS

We presented results of computer simulations for the electron transmission through the two-dimensional rings which have square and circular forms with two terminals. The results show that taking into account of the second dimension plays the principal role in the electron transport, independently of the ring's aspect ratio defined as a ratio between the width of the ring's arms and its size d/L. This conclusion was also made for the closed two-dimensional rings.[55,56] Only for very low energies of an incident electron when the single-channel transmission takes place, the electron transport is laminar provided that the flux is zero. If the electron transport in the two-dimensional structure remained laminar with increasing energy or application of the flux, the second dimension would lead to the fluctuation of the phase of the electron trajectories, in dependence of what flux is enclosed by these trajectories in the ring. Consequently, we obtained the aperiodical ABO's of the transmission with aperiodicity proportional to the width of the ring's arms.[16] In reality, our

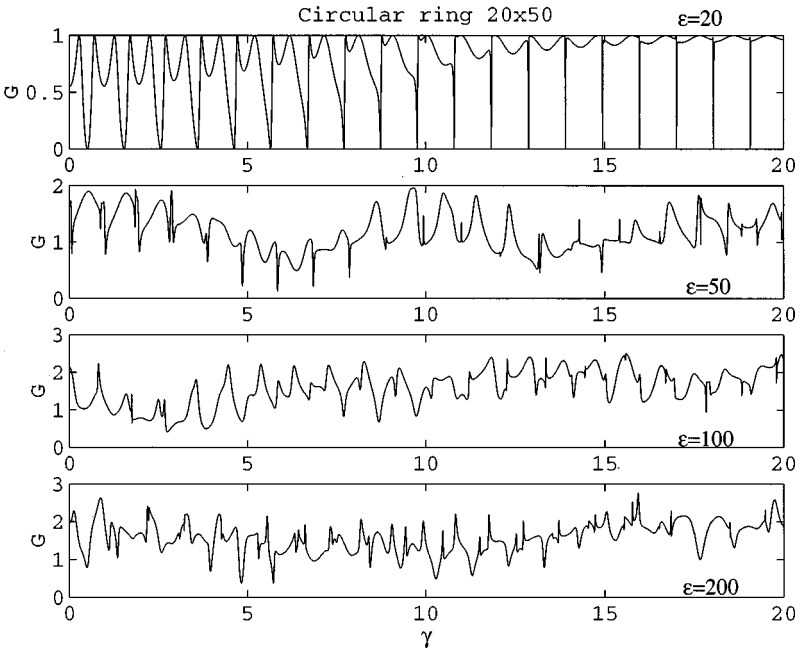

FIG. 13. The same as in Fig. 12 with a moderate aspect ratio $d/L=0.25$ (the 20×50 circular ring).

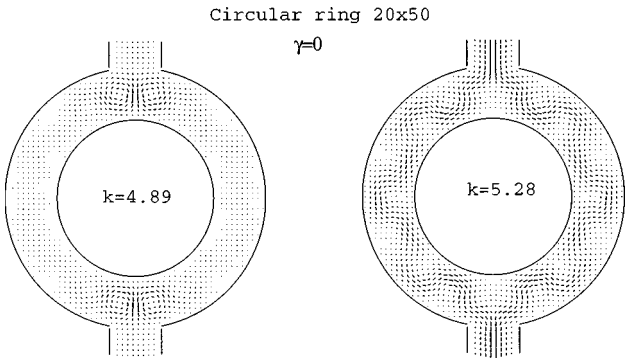

FIG. 14. Evolution of probability current distributions from the laminar regime to a convectional one with an increase in energy of incident electron in the circular ring.

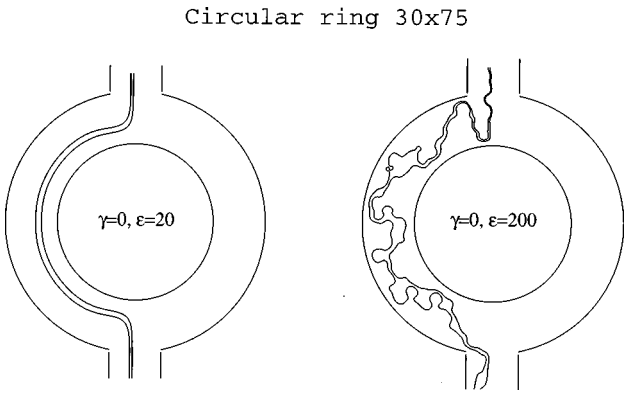

FIG. 15. The quantum-mechanical streamlines which are analogous to the classical trajectories for the single-channel (left) and four-channel transmissions (right). In both cases the numerically closest incident trajectories are taken in the input lead.

computer simulations of the current flow patterns reveal that as soon as the flux is applied or the energy of the incident electron increases, the electron trajectories may form the vortex structure. For the single-channel transmission a single vortex forms near the entrance to the ring (see Figs. 5, 11, and 14) which equalizes the flux induced phases for the different electron trajectories. As a result, we have the regular quasiperiodical ABO's in the flux region determined by the aspect ratio of the ring (see Figs. 1–3, 12, and 13) with a periodical set of zeroes of the transmission. That result does not depend on the geometrical form of the rings. However, the character of the ABO's in the case of the single-channel transmission substantially depends on the energy of the incident electron. If the energy of the incident electron slightly exceeds the even quasienergies of the ring, the eigenfunctions of which have the same symmetry as the symmetry of the incident wave function with respect to $y \rightarrow -y$ for zero flux, we obtain the almost sinusoidal ABO's (Fig. 10, the third subplot). Otherwise, the ABO's contain two harmonics (Fig. 10, the fourth subplot).

In a real semiconductor and especially in metal ring structures we deal with the multichannel transport of electrons. The nodal lines of the wave function inside the ring are defined both by azimuthal and radial quantum numbers. Correspondingly, the current distribution pattern becomes convectional. These convectional patterns look like a quasiregular vortex lattice with the period strongly dependent on the energy of the incident electron (or on the number of channels) provided that the flux is zero. The elementary cell of the vortex lattice may be simply vortex or may be very complicated consisting of a few vortices and antivortices as it is shown in Fig. 14 for the circular ring.

Application of the flux strongly distorts the convectional current flow patterns partially destroyng the vortex lattice. Moreover, the lattice elementary cell may undergo enormous changes. It leads to strong flux phase shift differences for different electron trajectories. In this case even the closest electron trajectories at the entrance of the ring may get the finite phase shift difference as it is shown in Fig. 15. If the distance between entrance trajectories is equal to the numerical lattice unit, at the moment of exit these trajectories can get the phase difference of order fL, where L is a characteristic scale of the structure and f is the channel's number. As a result, the ABO's of the transmission or the conductance become irregular as one can see from Figs. 1–3, 12, and 13. Thus the current and streamline patterns illustrate the origin of large nonuniversal conductance fluctuations which may be due to both quantum interference because of, e.g., coherent backscattering and the particular geometry of the ring.[54] A level of backscattering processes strongly depends on energy of an incident electron.

Thus, the current and streamline patterns shown in Figs. 5, 6, 11, 14, and 15 reveal the important role of the convectional regime and vortices in the electron current flow which make the phase differences many times as large as the ring scale L. That may serve as an interpretation of irregularity of the Aharonov-Bohm oscillations for multichannel electron transport. The reason for this is complicated packing of nodal lines and points inside the ring for the multichannel transmission.

ACKNOWLEDGMENTS

The authors wish to express their gratitude to Petr Ĉheba for stimulating discussions and Karl-Fredrik Berggren for providing original results of his investigations. Also we are indebted to our collegues from Laboratory of Theory Nonlinear Processes Kirill Alekseev, Andrey Kolovskii and especially Evgeny Bulgakov for many helpful discussions. Support of INTAS-RFBR Grant No. 95-657 and RFFI Grant No. 97-02-16305 is acknowledged.

*Electronic address: zeos@zeos.krascience.rssi.ru

[1] For a review see *Physics of Nanostructures*, edited by J. H. Davies and A. R. Long (Institute of Physics, Bristol, 1992).

[2] Y. Aharonov and D. Bohm, Phys. Rev. **115**, 485 (1959).

[3] W. Franz, Phys. Ber. **41**, 686 (1940).

[4] B.I. Al'tshuler, A.G. Aronov, and B.Z. Spivak, Pis'ma Zh. Éksp. Teor. Fiz. **34**, 101 (1981) [JETP Lett. **34**, 94 (1981)].

[5] Y. Gefen, Y. Imry, and M.Ya. Azbel, Phys. Rev. Lett. **52**, 129 (1984).

[6] Y. Gefen, Y. Imry, and M.Ya. Azbel, Surf. Sci. **142**, 203 (1984).

[7] M. Buttiker, in *SQUID '85, Superconducting Quantum Interference Devices and their Applications*, edited by H.D. Hahlbohm and H. Lubbig (Walter de Gruyter, New York, 1985), p. 529.

[8] E.N. Bulgakov and A.F. Sadreev, Phys. Rev. B **52**, 11 938 (1995).
[9] J.P. Carini, K.A. Muttalib, and S.R. Nagel, Phys. Rev. Lett. **53**, 102 (1984).
[10] D.A. Browne, J.P. Carini, K.A. Muttalib, and S.R. Nagel, Phys. Rev. B **30**, 6798 (1984).
[11] M. Büttiker, Y. Imry, R. Landauer, and S. Pinhas, Phys. Rev. B **31**, 6207 (1985).
[12] R.A. Webb, S. Washburn, C.P. Umbach, and R.B. Laibowitz, Phys. Rev. Lett. **54**, 2696 (1985).
[13] R.A. Webb, S. Washburn, C.P. Umbach, and R.B. Laibowitz, in *SQUID '85, Superconducting Quantum Interference Devices and their Applications* (Ref. 7), p. 56.
[14] R.A. Webb, in *Quantum Coherence* (World Scientific, Singapore, 1990).
[15] S. Washburn and R.A. Webb, Adv. Phys. **35**, 375 (1986).
[16] A.D. Stone, Phys. Rev. Lett. **54**, 2692 (1985).
[17] J. Skjånes, E.H. Hauge, and G. Schön, Phys. Rev. B **50**, 8636 (1994).
[18] M.Ya. Azbel, A. Hartstein, and D.P. Di Vincenzo, Phys. Rev. Lett. **52**, 1641 (1984).
[19] J.K. Jain and S.A. Kivelson, Phys. Rev. Lett. **60**, 1542 (1988).
[20] J.K. Jain and S.A. Kivelson, Phys. Rev. B **37**, 4111 (1988).
[21] B. Shapiro, J. Phys. C **19**, 4709 (1986).
[22] A.M. Chang, G. Timp, T.Y. Chang, J.E. Cunninghamn, P.M. Mankiewich, R.E. Behringer, and R.E. Howard, Solid State Commun. **67**, 769 (1988).
[23] A.M. Dirac, Proc. R. Soc. London, Ser. A **133**, 60 (1931).
[24] J.O. Hirschfelder, A.C. Christoph, and W.E. Palke, J. Chem. Phys. **61**, 5435 (1974).
[25] J.O. Hirschfelder, C.J. Goebel, and L.W. Bruch, J. Chem. Phys. **61**, 5456 (1974).
[26] J.O. Hirschfelder, J. Chem. Phys. **67**, 5477 (1974).
[27] S. Bandyopadhyay, S. Chaudhuri, B. Das, and M. Cahay, Superlattices Microstruct. **12**, 123 (1992).
[28] S. Chaudhuri, S. Bandyopadhyay, and M. Cahay, Superlattices Microstruct. **11**, 241 (1992).
[29] S. Chaudhuri, S. Bandyopadhyay, and M. Cahay, Phys. Rev. B **47**, 12 649 (1993).
[30] K.-F. Berggren, C. Besev, and Zhen-Li Ji, Phys. Scr. **T42**, 141 (1992).
[31] K.-F. Berggren and Zhen-Li Ji, Phys. Rev. B **47**, 6390 (1993).
[32] H. Wu and D.W.L. Sprung, Phys. Rev. A **49**, 4305 (1994).
[33] H. Wu, D.W.L. Sprung, and J. Martorell, Phys. Rev. B **45**, 11 960 (1992).
[34] C.S. Lent, Phys. Rev. B **43**, 4179 (1991).
[35] M. Leng and C.S. Lent, Superlattices Microstruct. **11**, 351 (1992).
[36] V.M. Ramaglia, F. Ventriglia, and G.P. Zucchelli, Phys. Rev. B **48**, 2445 (1993).
[37] V. Marigliano Ramaglia, F. Ventriglia, and G.P. Zucchelli, Phys. Rev. B **52**, 8372 (1993).
[38] M. Shin, K.W. Park, S. Lee, and Ei-Hang Lee, Phys. Rev. B **53**, 1014 (1996).
[39] R. Landauer, Philos. Mag. **21**, 863 (1970).
[40] M. Buttiker, Phys. Rev. B **38**, 9375 (1988).
[41] H. Kasai, K. Mitsutake, and A. Okiji, J. Phys. Soc. Jpn. **60**, 1679 (1991).
[42] K. Vacek, A. Okiji, and H. Kasai, Phys. Rev. B **47**, 3695 (1993).
[43] R.L. Schult, H.W. Wyld, and D.G. Ravenhall, Phys. Rev. B **41**, 12 760 (1990).
[44] Y. Avishai and Y.B. Band, Phys. Rev. Lett. **62**, 2527 (1989).
[45] L.L. Chang, L. Esaki, and R. Tsu, Appl. Phys. Lett. **24**, 593 (1974).
[46] J.P. Bird, D.M. Olatona, R. Newbury, R.P. Taylor, K. Ishibashi, M. Stopa, Y. Aoyagi, T. Sugano, and Y. Ochiai, Phys. Rev. B **52**, R14 336 (1995).
[47] J. Appenzeller, Th. Schäpers, H. Hardtdegen, B. Lengeler, and H. Lüth, Phys. Rev. B **51**, 4336 (1995).
[48] K.N. Pichugin and A.F. Sadreev, Zh. Éksp. Teor. Fiz. **109**, 546 (1996) [JETP **82**, 290 (1996)].
[49] A.F. Sadreev and V.A. Vid'manov, Int. J. Mod. Phys. B **9**, 2719 (1995).
[50] E.N. Bulgakov and A.F. Sadreev, Phys. Low-Dim. Struct. **1/2**, 33 (1997).
[51] M. Büttiker, Y. Imry, and M.Ya. Azbel, Phys. Rev. A **30**, 1982 (1984).
[52] E.A. Jagla and C.A. Balseiro, Phys. Rev. Lett. **70**, 639 (1993).
[53] M. Di Ventra, F. Gagel, and K. Maschke, Phys. Rev. B **55**, 1353 (1997).
[54] Zhen-Li Ji and K.-F. Berggren, Phys. Rev. B **52**, 1745 (1995).
[55] W.-C. Tan and J.C. Inkson, Phys. Rev. B **53**, 6947 (1996).
[56] I. Tomita and A. Suzuki, Phys. Rev. B **53**, 9536 (1996).